Wear 560–561 (2025) 205607

Contents lists available at ScienceDirect

Wear

journal homepage: www.elsevier.com/locate/wear

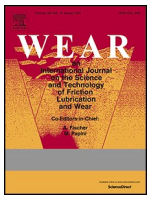

A novel procedure to predict cumulative tool wear in turning based on experimental analysis

Andrea Abeni [a,*], Aldo Attanasio [a], José Outeiro [b,c], Gerard Poulachon [b]

[a] University of Brescia, Department of Mechanical and Industrial Engineering, Brescia, Italy
[b] Arts et Metiers Institute of Technology, LABOMAP, Université Bourgogne Franche-Comté, HESAM Université, Cluny, France
[c] Department of Mechanical Engineering and Engineering Science, University of North Carolina at Charlotte, Charlotte, NC, 28223, USA

ARTICLE INFO

Keywords:
Cumulative tool wear
Turning
AISI 1045
Useful tool-life
Tool substitution policy

ABSTRACT

Tool wear is one of the most challenging issues in manufacturing. In cutting processes, tool-life testing procedures are defined by ISO standards. These standards give the guidelines to perform tool-life testing in terms of workpiece material, tool geometry, tool material, cutting fluid, tool wear assessment, and tool-life evaluation. For determining the useful tool-life, the standards recommend running several tool-life tests at constant cutting speed till reaching a specified value of tool wear, as defined by the selected tool-life criterion. But, in industrial applications, the approach is different. The same tool is often used to make different geometrical features on the same component using different process parameters, depending on the desired geometry and surface quality. Therefore, it is possible to state that the tool accumulates wear over the working time under different cutting conditions. In other words, the tool is subjected to cumulative tool wear. This paper aims to deepen the knowledge about cumulative tool wear, which means the tool wear generated by a combination of different process parameters. An innovative experimental procedure is proposed to determine the useful tool-life when machining a part with the same tool at different process parameters. Cumulative tool flank wear tests were performed on AISI 1045 samples by changing the cutting speed, keeping the other cutting parameters constant. The experimental cumulative flank wear evolution was compared with the theoretical one. Four different machining cycles were tested to simulate different industrial cases. The comparison revealed a good agreement between the prediction and the experimental data.

1. Introduction

Tool wear in metal cutting is a complex phenomenon with a pre-eminent role in the industry's tool management policies. An accurate estimation and maximization of the tool-life is essential to improve both the efficiency and sustainability of machining operations [1]. At the same time, the geometrical evolution of the tool due to wear impacts part dimensional accuracy, surface integrity issues, and the overall quality of the machined parts [2,3]. Monitoring tool wear is a challenging and time-consuming task, regulated by some technical standards. The reference International Standards are ISO 3685: 1993 [4] for single-point turning tools, ISO 8688-1: 1989 [5] for face milling, and ISO 8688-2: 1989 [6] for end-milling.

They all suggest monitoring the progress of the wear during machining, by periodically interrupting the test to perform some direct measurements of some geometrical features of the tool which are affected by wear. Tool flank wear width (VB) and the geometry of the crater wear on the tool rake surface (position and depth) are the parameters commonly used to evaluate tool wear evolution for cemented carbide cutting tools [7–9]. The tool-life procedure reported in the ISO standards is based on tests performed at constant cutting conditions during the entire duration of the test. In particular, Constant Cutting Speed (CCS) tests must be executed to measure the evolution of tool wear parameters in function of the time. The outputs of the CCS tests are tool wear versus time plots (Fig. 1). The shape of these plots is characterised by three different zones. At the beginning of the process, when the tool is new, the wear rate ($\frac{dW}{dt}$ in Fig. 1) is high but it rapidly decreases (zone I, called running-in or break-in period), and it reaches a constant value during the steady wear zone (zone II) [10]. At the end of the tool-life (the zone III, called accelerated wear zone), the wear rate increases, determining a rapid deterioration of the cutting tool [11]. Then, the useful tool-life is calculated as the time at which the tool-life

* Corresponding author.
E-mail address: andrea.abeni@unibs.it (A. Abeni).

https://doi.org/10.1016/j.wear.2024.205607
Received 25 July 2024; Received in revised form 1 October 2024; Accepted 17 October 2024
Available online 18 October 2024

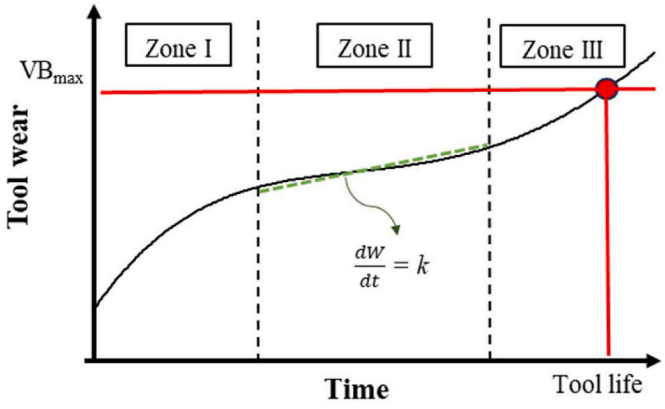

Fig. 1. Example of the evolution of tool wear in function of the time.

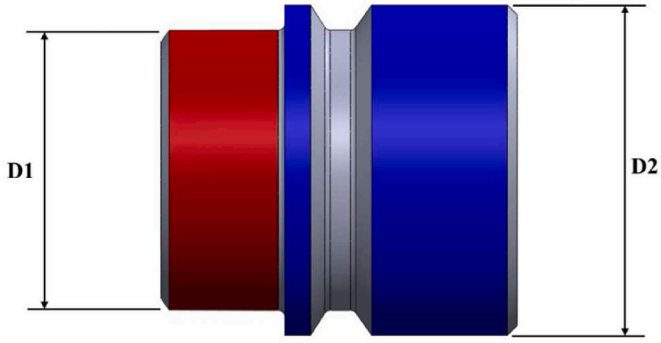

Fig. 2. Detail of a compressed air connector.

parameter reaches a defined limit value defined by the tool wear criterion. Several tests can be performed by changing the process conditions in order to evaluate the impact of the parameters on wear. Cutting speed has a considerable effect on the tool wear rate.

Analytical or numerical tool wear models require the instantaneous tool wear rate ($\frac{dW}{dt}$ in Fig. 1) to accurate predict the tool wear evolution in function of the time and tool-life [12]. Consequently, the time-dependent effect of wear on tool geometry should be considered to investigate the impact of process parameters on tool-life. One of the most interesting and low-investigated factors is the non-linear effect of the cutting speed on tool wear. The use of non-constant cutting speed is common in industrial applications. For example, considering the industrial case of a fast connection system shown in Fig. 2, the cylindrical surfaces highlighted with red and blue shaded areas are manufactured using the same tool. The feed and the depth of cut used to generate these features should be constant. Their values are set considering the allowance and the final roughness required by the designer. On the other hand, the CNC machine tools used to produce large batch sizes are usually programmed to work at constant rotational spindle speed to avoid the generation of vibrations due to the change of the spindle speed. Due to the differences between the diameters (D1 and D2 in Fig. 2) of the surfaces to be manufactured, the cutting speed will be different.

In these cases, the tool-life estimation cannot be done by applying the ISO standard 3685 [4], since the tools are submitted to different cutting speeds, generating cumulative tool wear effect induced by different cutting speeds. Several studies [13–17] investigated the effects of the cutting speed on tool wear, but most of them did not consider the effects of changing the cutting speed during machining operations performed with the same tool. A theoretical background about cumulative damage was outlined in 1945 by Miner [18] with the hypothesis to describe the fatigue phenomenon by employing linear models. Palmai [19] was the first to explore the effects of the variation of the cutting speed on tool wear evolution. he hypothesis of linearity was expressed by equation (1), valid for machining under different cutting speeds v_i for intervals of time Δt_i. T_i is the tool-life pertaining to the constant cutting speed v_i.

$$\sum_{i=1}^{N} \frac{\Delta t_i}{T_i} \cong 1 \tag{1}$$

The theoretical discussion of the hypothesis was supported by the experimental validation reported in Ref. [20]. The tests consisted of longitudinal turning of rolled AISI 1045 steel and can be classified into two groups by considering their purpose.

Group 1) tests made to calculate the tool-life T_i at two different cutting speeds (*cutting* $v_{c1} < v_{c2}$), performing Constant Cutting Speed (CCS) tests according to ISO standards.
Group 2) tests made to quantify the effect of the non-linearity of wear phenomena on useful tool-life prediction, performing Variable Cutting Speed (VCS) tests. All the machining tests performed by Palmai started setting the highest cutting speed (v_{c2}), then, according to the design of experiments, the cutting speed was decreased to v_{c1} until reaching the limit value of the tool-life criterion. Therefore, seven tests were performed by varying the instant of speed reduction. For each test, the hypothesis of linearity was verified by using equation (1). The values of summations ranged between 0.77 and 1.26. In Ref. [21] the same procedure was applied to an increased number of VCS tests performed with 3 changes of cutting speed for each test, achieving similar results. In both cases, an equivalent cutting speed v_{ce} was computed as the constant speed determining the same tool-life of a determined cutting speed cycle. The computation of v_{ce} was executed assuming a neglectable contribution of the non-linear effects, while the equivalent tool-life T_e was computed with the Taylor formulation as a function of v_{ce}. The results showed a meaningful difference between the useful tool-life achieved during the experimental VCS tests ($\Delta t_1 + \Delta t_2 + \Delta t_3$) and the predicted one (T_e).

The main drawback of this approach is that his validity is based on the assumption of linear correlation between tool wear and cutting time. It is important to highlight that the useful tool-life is the result of tool wear evolution in all the three zones illustrated in Fig. 1. Wear versus time curve is not a straight line, but a monotonically non-decreasing function composed by three different curves.

Furthermore, research works [19–21] focused only on the useful tool-life, and the effect of non-linearity on the evolution of VB during time was not considered. As a consequence, the possibility of neglecting non-linearity effects in industrial application of tool wear monitoring remained uncertain.

Jemielniak et al. [22] investigated the cumulative tool wear by varying cutting speed and feed in turning plain carbon steel. The research pointed out that with uncoated cemented carbide tools the non-linear effect was negligible, while with TiC-TiN coated carbide tools the wear development depended on the actual sequence of process parameters. The measurement of tool wear was performed just when the process parameters (i.e. cutting speed and feed) changed. As a consequence, the results are strongly affected by the high uncertainty due to the limited experimental data. A robust statistical approach is necessary, especially to fully analyse the zone III of the tool-life curve, when the increasing wear rate leads to a rapid development of the tool wear. Hung and Zhong [23] verified the validity of the linearity hypothesis about cumulative wear in longitudinal and face turning operations on metal matrix composites. Oija and Dixit [24] used artificial neural networks to study the influence of the cutting speed on tool-life in turning plain carbon steel. Based on the hypothesis of linearity of cumulative effects, they achieved a good prediction in most of the cases, although in some tests a considerable error of the model is observed. In order to limit the regenerative effects of chatter vibrations, Albertelli et al. [25] studied

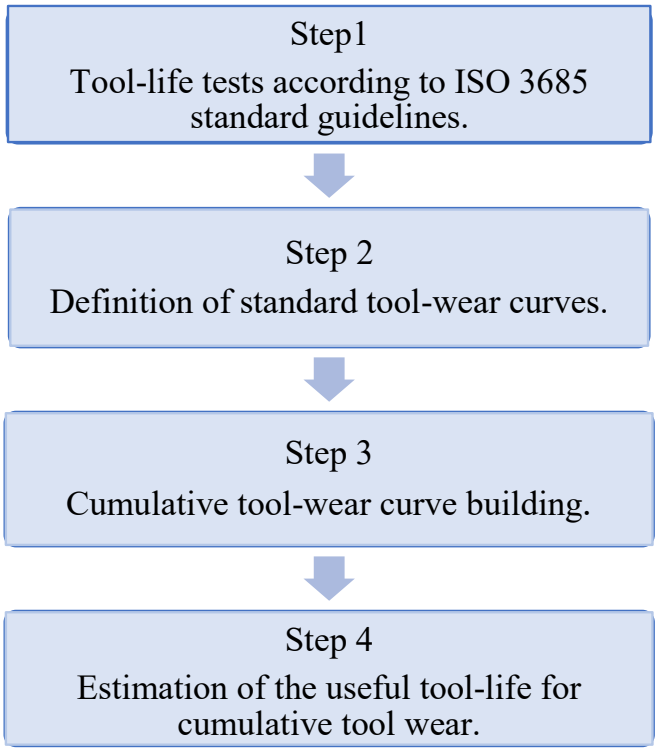

Fig. 3. New procedure for the estimation of the tool-life when cumulative tool wear is present.

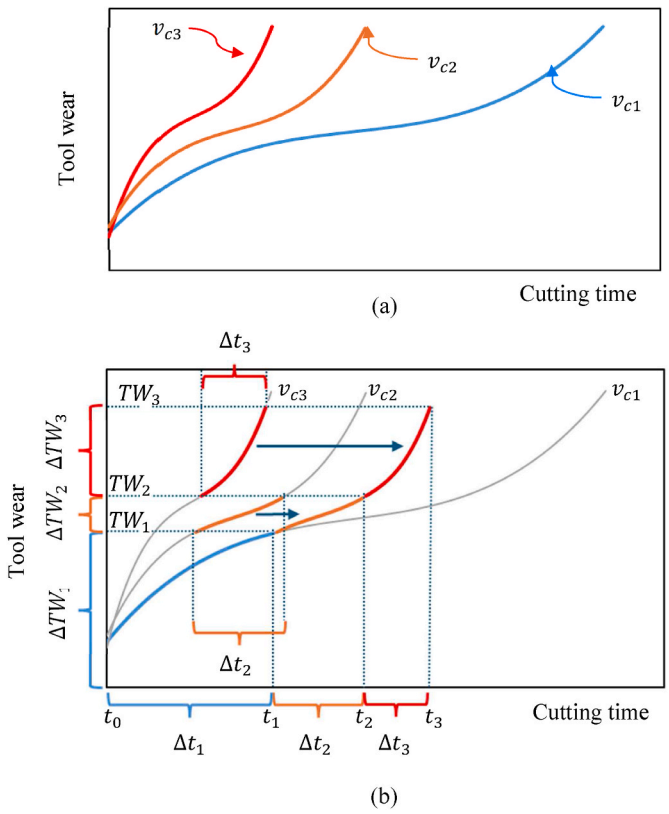

Fig. 4. (a) Example of tool wear curves; (b) building of the empirical cumulative tool-wear curve.

how the continuous modulation of the spindle speed affects the tool wear, and how it negatively impacts the tool-life.

In general, the literature shows contradictory conclusions about the linearity of cumulative tool wear. Therefore, the study of cumulative tool wear required a robust statistical approach based on frequent and repeated evaluation of the wear to distinguish between the effects of non-linearity and the intrinsic variability of the damage phenomena. This paper aims to.

1) Verify that the non-linear effects have a marginal impact on the evolution of tool wear in function of the time.
2) Establish an innovative procedure to determine the tool-life when using variable cutting speed.

The proposed procedure is applied to longitudinal turning of AISI 1045 steel using coated carbide tools. In order to reduce the uncertainties related to the variability of unknown factors, the work material is characterised in terms of its microstructure and hardness. CCS tests were performed with three different cutting speeds by repeating each test three times to statistically describe the evolution of VB in function of the time. The paper describes in detail how the procedure allows to obtain the empirical curves of cumulative tool wear. Finally, VCS tests were performed using different combinations of cutting speed to validate the procedure. The comparison between predicted and experimental results highlights the actual impact of non-linear effects.

The proposed procedure can be easily applied in industrial environments, regardless the workpiece material, the tool material and geometry, the lubrication, and the process parameters.

2. Procedure for estimating tool-life based on the cumulative tool wear concept

As already discussed in the introduction, often in industrial practice the estimation of the tool-life cannot be done just applying the ISO standard 3685, since the tools are alternatively subjected to different cutting speeds generating cumulative tool wear (see Fig. 2). It is in this context that a new procedure for a reliable evaluation of the tool-life when the cutting process is characterised by cumulative tool wear was developed. The proposed procedure merges the ISO 3685 standards guidelines, where tool-life tests are performed at constant cutting speed, and the industrial practice, where the same tool is used to manufacture different features on the same component using different cutting conditions.

Fig. 3 shows the flowchart of the proposed procedure, composed by four steps.

In the first step, tool-wear tests are performed according to ISO 3685 standard guidelines to obtain wear data. Tool geometry, tool material, work material, and process parameters are the same as the analysed industrial machining process. In particular, cutting speeds are selected considering the working cycle of the industrial part. Each test must be repeated at least three times for statistical analysis.

Starting from the collected wear data, the tool-wear curve for each cutting speed is defined as the average of three tool-wear curves from tool-life tests (step 2).

These curves are essential to build the cumulative tool-wear curve (step 3). In fact, the empirical curve representing the cumulative wear of the tool is constructed by combining the standard tool-wear curves and taking into account the working cycle of the part.

Fig. 4 shows how the cumulative tool wear curve is built starting from standard tool-wear curves (Fig. 4a) obtained using three different cutting speeds and considering a working cycle of three phases (Fig. 4b).

- Phase 1: to manufacture a first feature setting a low cutting speed (v_{c1}) for an interval of time $\Delta t_1 = (t_1 - t_0)$, and a cumulative tool wear equal to $\Delta TW_1 = TW_1$;
- Phase 2: to manufacture a second feature setting an intermediate cutting speed (v_{c2}) for an interval of time $\Delta t_2 = (t_2 - t_1)$, and a cumulative tool wear equal to $\Delta TW_2 = (TW_2 - TW_1)$;

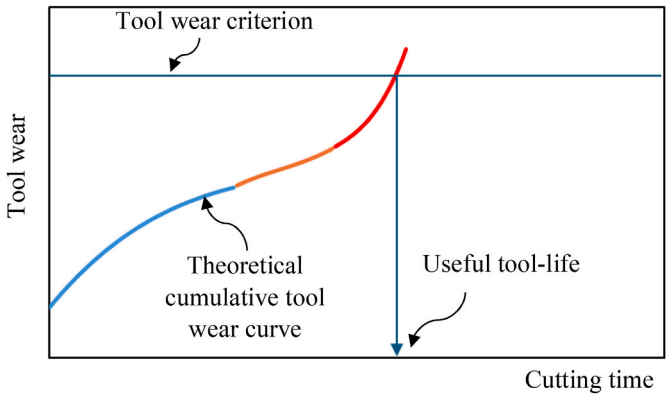

Fig. 5. Estimation of the useful tool-life for cumulative tool wear.

- Phase 3: to manufacture a third feature setting a high cutting speed (v_{c3}) for an interval of time $\Delta t_3 = (t_3 - t_2)$, and a cumulative tool wear equal to $\Delta TW_3 = (TW_2 - TW_3)$.

The empirical cumulative tool wear curve is built as follows.

1. The first part of the curve (blue line in Fig. 4b) corresponds to the initial portion (between t_0 and t_1) of the standard tool wear curve related to v_{c1}. The tool wear at the end of the first phase is TW_1.
2. The second part of the curve (orange line in Fig. 4b) is drawn translating along the time axis the portion of the standard tool wear curve related to v_{c2} starting from TW_1 and included in an interval time equal to Δt_2. The tool wear at the end of this phase is TW_2.
3. Similarly, the third part of the curve (red line in Fig. 4b) is drawn translating along the time axis the portion of the standard tool wear curve related to v_{c3} starting from TW_2 and included in an interval time equal to Δt_3.

The last step of the procedure (step 4) estimates the useful tool-life for cumulative tool wear. As shown in Fig. 5, according to the selected tool-life criterion, it is possible to estimate the useful tool-life for cumulative tool wear from the theoretical cumulative tool wear curve.

3. Experimental methods

Experimental turning tests were performed to validate the procedure described in the previous section. The tests consist of longitudinal turning performed on AISI1045 samples at constant feed and at variable cutting speed. According to the standard ISO 3685: 1993, at least three different cutting speeds shall be chosen, in order to ensure the tool-life at the highest speed is not less than 5 min.

Flank wear width (*VB*) was employed as tool-life criterion, and it was monitored by using a multifocal optical microscope. The chemical composition, hardness and microstructure were characterized in order to check the homogeneity of the workpiece material.

3.1. Characterisation of the work material

The samples used in the experimental tests were obtained from the same batch of AISI 1045 hot rolled bars provided by Ascométal France Holding SAS. The chemical composition of the work material was quantified using the spectrometer Horiba Jobin Yvon JY3. Before measuring the chemical composition, the spectrometer was calibrated by means of the reference sample made of SS407 steel. Measurements were done on samples randomly collected from the material batch and they were repeated on two samples. Five measurements per sample were performed.

Brinell hardness (HB) tests were performed using a load of 187.5 Kg and a tungsten carbide spherical indenter with a diameter of 2.5 mm

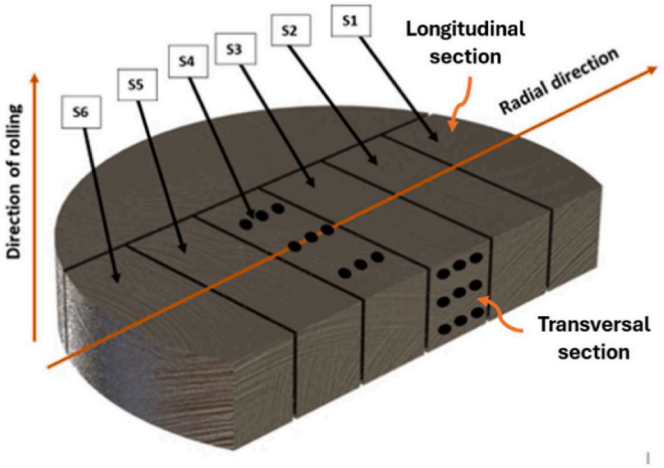

Fig. 6. Pattern of the micro-hardness tests.

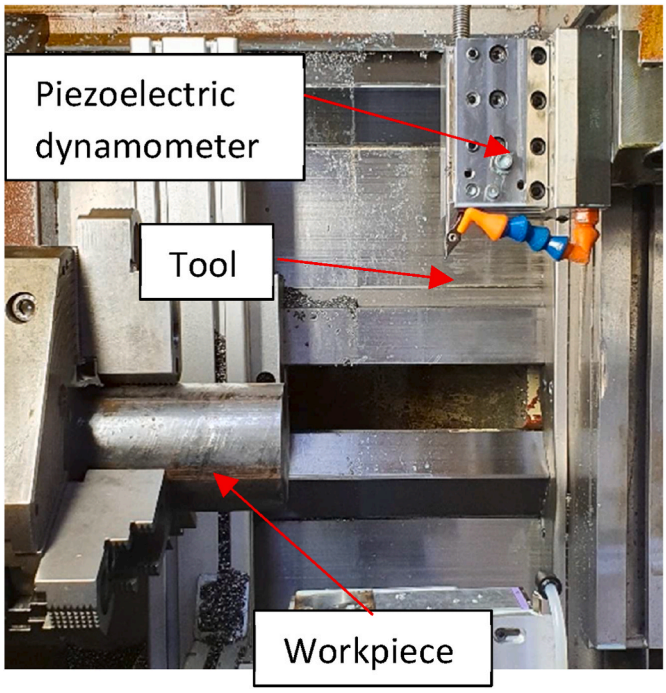

Fig. 7. Experimental setup (Sonim T9 at LaBoMaP of Cluny Arts et Métiers Institute of Technology).

using an Instron Wolpert Tester. The same samples employed for the chemical composition analysis were utilized, as schematised in Fig. 6, to cut six specimens from each sample, for a total of twelve samples.

Since a non-uniformity of the material hardness could affect the results of the tests, the homogeneity of the provided work material was checked measuring the hardness along the radial direction on two surfaces: i.e., the surface that is orthogonal to the bar axis, and the surface that contains the bar axis. Nine measurements on each surface were done (see Fig. 6).

The same samples used for the hardness measurements were used for the metallographic analysis of the material. This analysis was performed.

- to measure the grain size of the material.
- to check the homogeneity of the material microstructure from the external surface to the axis of the bar.
- to find the presence of any defects such as inclusions, and cracks.

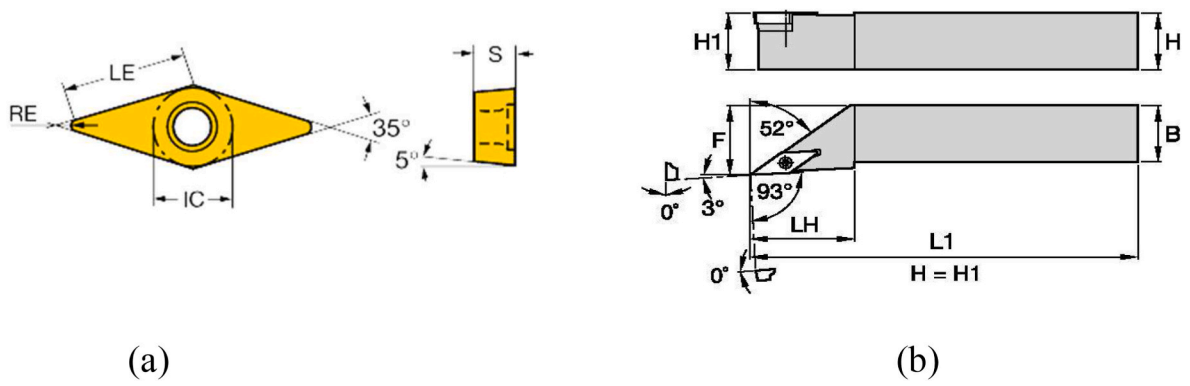

Fig. 8. (a) VBMT 160404 insert; (b) SVJBR 2020K16 tool holder.

Each sample was incorporated in a conductive resin, and it was polished to a mirror-like finishing. Then, Nital (4 % HCl + 96 % Ethanol) was selected as etching agent, and applied on the sample surface for 5 s at room temperature. In this manner, the microstructure was revealed. The surfaces were finally observed with an Olympus BX51M optical microscope at different magnifications (2.5×; 5x; 20x; 50x) to observe this microstructure, such the grain morphology and the phases.

3.2. Machining tests

Longitudinal turning tests were performed on two different CNC lathes, namely a Sonim T9, available at LaBoMaP of the Cluny Campus of Art et Métiers Institute of Technology, equipped with a spindle of 30 kW and a maximum rotational speed of 4000 RPM, and OCN-PPL Olimpus, available at the Technology and Manufacturing Systems Laboratory of the University of Brescia, equipped with a spindle of 7.5 kW and a maximum rotational speed of 6000 RPM. Both lathes use 840D Siemens CNC controller. The use of two different machine-tools permitted to verify if the lathe features (i.e., stiffness, jaw chuck, spindle, …) affect the tool wear. Fig. 7 shows the experimental setup.

The longitudinal turning operations were performed using Sandvik VBMT 160404 p.m.4325 insert (Fig. 8a) mounted on the Kennametal tool holder SVJBR 2020K16 (Fig. 8b). As shown in Fig. 8, the tool geometry is characterised by a normal rake angle (γ) equal to 0°, a normal clearance angle (α) equal to 5°, and a tool cutting edge angles of the major cutting edge (κ) equal to 93°.

The inserts are made of coated tungsten carbide with a triple CVD coating (TiCN-Al2O3-TiN). The actual cutting-edge radius was measured using the Mitaka PF-60 autofocus laser profilometer, obtaining a value equal to 0.040 ± 0.003 mm.

The workpieces were cylindrical bars with an initial diameter of 80 mm and initial length of 120 mm. The bars were machined until a final diameter of 40 mm. Cutting forces were measured by a piezoelectric dynamometer from Kistler model 9121, characterised by a measuring accuracy of 0.01 N.

According to the first step of the procedure, tool-life tests were performed in agreement with ISO 3685 standard. Therefore, tool-life tests at constant cutting speed were conducted. Subsequently, four VCS tool-life tests were executed by varying the cutting speed during each test. To correctly replicate the production practice, the experimental tests were run setting a machining cycle which alternates short cuts of 5 s to long pause of 60 s. The cycle was repeated up to reach the instants defined for tool wear measurement.

Three different cutting speeds equal to $v_c = 300$ m/min, $v_c = 350$ m/min, and $v_c = 400$ m/min were selected to obtain the basic curves describing the wear behaviour for the investigated tool-material pair. Cutting speed values were chosen considering the cutting speed suggested by the tool manufacturer for AISI 1045 cutting and guaranteeing that the tool-life at the highest speed (i.e., $v_c = 400$ m/min) was not less than 5 min. All the other process parameters were kept constant. The feed (f) was set equal to 0.1 mm/rev, the depth of cut (a_p) equal to 1 mm, and standard cutting fluid composed by a mixture of 5 % of oil (Zubora 65 M) and water was used. It was applied with a nozzle in the area of contact between the tool and the workpiece with a pressure of 0.8 bar and a fluid flow of 75 l/min. To verify the repeatability of the experiments and for statistical analysis, each test was carried out three times. The first repetition of each test was performed with lathe Sonim T9, while the second and third with lathe OCN-PPL Olimpus.

3.3. Tool wear monitoring

The tool flank wear was monitored using the digital multi-focus

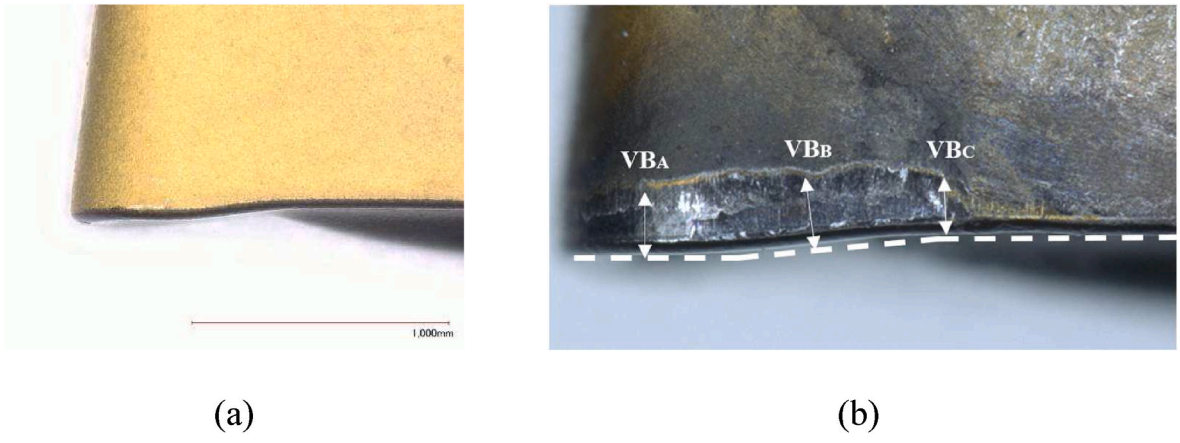

Fig. 9. (a) Profile of the VBMT insert; (b) VB measuring zones.

Table 1
Chemical composition of the work material measured by spectrometry.

C %	Cr %	Cu %	Mn %	Mo %	Ni %	P %	S %	Si %	V %	Fe %
0,479	0,153	0,078	0,720	0,027	0,051	0,004	0,034	0,037	0,002	Rest

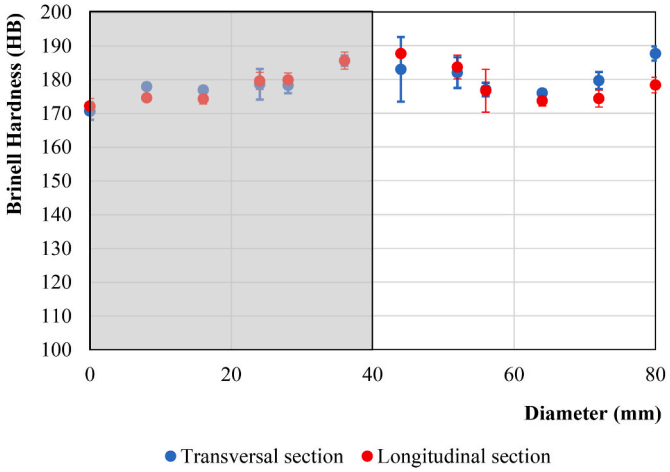

Fig. 10. Brinell hardness along the diameter measured along longitudinal and transversal sections.

microscopes Keyence VHX-1000 (measuring accuracy 1.0 μm) and Hirox RH2000 (measuring accuracy 0.8 μm). As suggested by the guidelines of ISO Standard 3685, being regular the observed flank wear land, an average width of VB equal to 0.3 mm was selected as tool-life criterion. Therefore, the tool-life tests were until reach the selected threshold value of VB. As shown in Fig. 9a, the tool cutting edge is not straight. Tool manufacturer optimised the shape of this insert for steel cutting in order to improve the final quality of the manufactured surfaces (i.e., the surface integrity), chip breaking, and tool-life. For this reason, it was decided to measure the flank wear in three different zones of the flank surface: one close to the end of the tool nose radius (VB_A); one along the inclined zone (VB_B); one along the straight zone (VB_C). Fig. 9b shows an example of flank wear measurement. The dotted line of Fig. 9b represents the profile of the unworn tool. For each measurement of VB, the unworn tool profile was overlapped with the worn profile to measure the extension of flank wear land, according to ISO Standard 3685.

The wear measurements were performed at the end of a tool pass, without stopping the machining while the insert was in contact with the workpiece. Furthermore, the number of passes between two consecutive measurements was not constant: it was decreased during the constant wear rate period and increased again in the accelerated wear zone to ensure a higher discretization of the curve in the portion were wear rate changes.

4. Results and discussion

4.1. Work material characterization

Table 1 shows the chemical composition of the work material measured by the spectrometer Horiba Jobin Yvon JY3. It was verified that the chemical composition corresponds to a standard AISI 1045 steel.

The work material hardness ranges from a minimum value of 168 HB and a maximum value of 190 HB with an average value equal to 179 HB and a global standard deviation of 5.4 HB.

Fig. 10 shows the mean values, and the corresponding standard deviation of the hardness measured along transversal and longitudinal sections as a function of the distance from the bar centre (diameter equal to 0). Observing Fig. 10, it is noticeable that, in general, the scattering of the hardness values along the bar section is low, and that, in particular, there is no evidence of any trend denoting a good homogeneity of the material hardness along the section. Only the hardness measured on the centre of the bar is slightly lower than the other hardness values. This behaviour can be explained considering the production cycle of the work material. The AISI 1045 bars provided by Ascométal France Holding SAS were manufactured by continuous casting and successive hot rolling mill process. The continuous casting process generates small cavities along the bar axis due to the material shrinkage during solidification.

Usually, these cavities are reduced in size or closed by hot rolling mill process, but a hardness reduction along the bar axis can be noticed. Additionally, during the cooling after the hot rolling mill process, the cooling rate of the bar core is lower than of the skin. Consequently, due to these phenomena a hardness reduction in the centre of the section is expected.

About the microstructure, the results of the analysis can be seen in Fig. 11. Samples 1, 2, and 3 show the microstructure on the longitudinal section; while samples 4, 5, and 6 show the microstructure of the transversal section (see Fig. 6). Sample 1 and 6, sample 2 and 5 and samples 3 and 4 were cut in symmetric positions around the centre of the bar because they are obtained at the same distance from the centre (averagely D = 13.3 mm for Sample 3 and 4, D = 40 mm for sample 2 and 4, D = 66.6 mm for samples 1 and 6). Standard AISI 1045 microstructure was observed. The work material microstructure is composed by equiaxed grains of ferrite (alfa-phase, white grains in Fig. 11), and grains of perlite, composed by lamellae of ferrite (white lamellae in Fig. 11), and cementite (black lamellae in Fig. 11).

By moving top-down in Fig. 11, it is possible to observe the changes in grain size in radial direction from the external part of bar (≈12.5 μm) to centre of the bar (≈24.3 μm). Observing the microstructures, it is also evident the effect of the rolling mill process on the material. Stretched grains in rolling direction (i.e., bar axis) are noticeable. Anyway, in order to avoid any type of effect of the grain dimension on the tool wear tests, it was decided to limit to 40 mm the minimum cutting diameter. This lower limit allows to set a maximum rotational speed of the spindle at 3183 RPM (D = 40 mm and cutting speed v_c = 40 m/min), which is lower than the maximum speed of lathe Sonim T9.

As shown in Fig. 12, the metallographic examination of sample 1 and 6, where the bar was machined during the tests, highlighted the presence of inclusions in the work material. These inclusions are uniformly distributed (as visible with magnification 5×), and their dimension is small ranging from 0.5 μm to 5 μm (as visible with magnification 50×), therefore their effect on the cutting test results can be neglected. In general, the material analysis showed a homogeneous material.

4.2. Validation of the procedure for useful tool-life estimation with cumulative tool wear

The procedure described in section 2 was applied and validated by experimental tests. In particular, firstly constant cutting speed tests with three different cutting speeds were performed to build the wear curves for AISI 1045. Once the wear curves were computed, they were used to define the theoretical cumulative tool wear curves and further tests were performed by changing the cutting speed accordingly.

4.2.1. Tool-life tests according to ISO 3685 standard

In this section, the results of constant cutting speed tool-life tests in agreement with ISO 3685 standard are described. As the standard suggests for sintered carbide tools, an average width of the flank wear land (VB) equal to 0.3 mm was selected as tool-life criterion. Fig. 13 shows

Longitudinal section	Transversal section
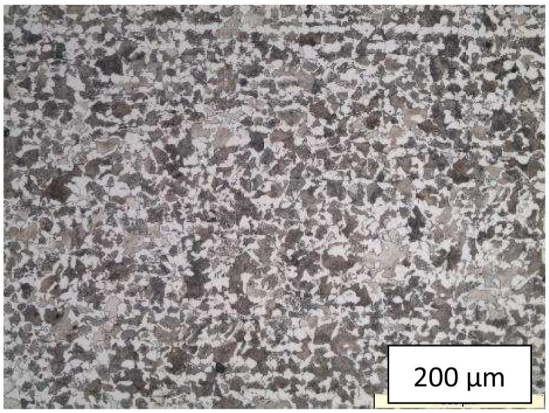	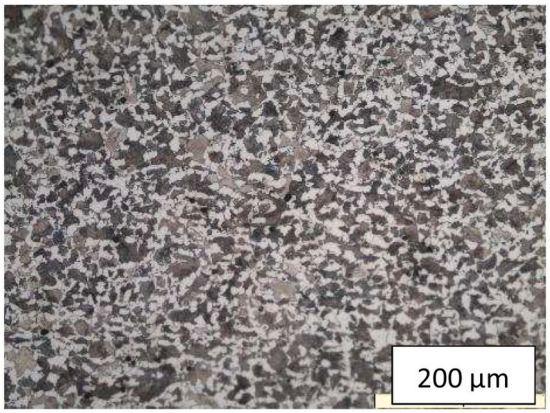
Sample 1 (D=66.7 mm; magnification 20x)	Sample 6 (D=66.7 mm; magnification 20x)
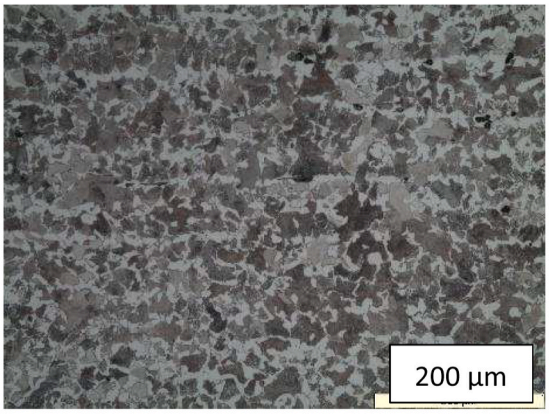	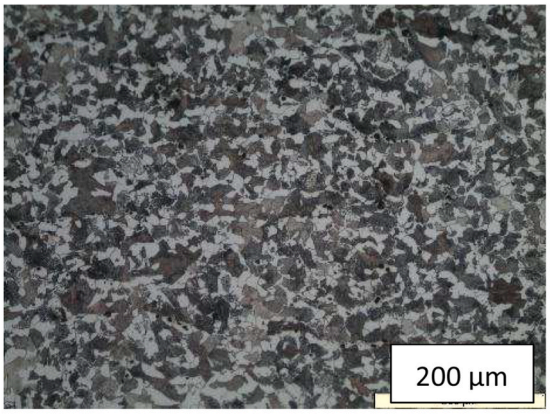
Sample 2 (D=40 mm; magnification 20x)	Sample 5 (D=40 mm; magnification 20x)
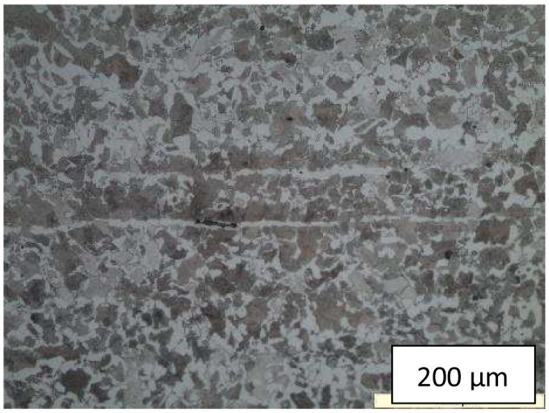	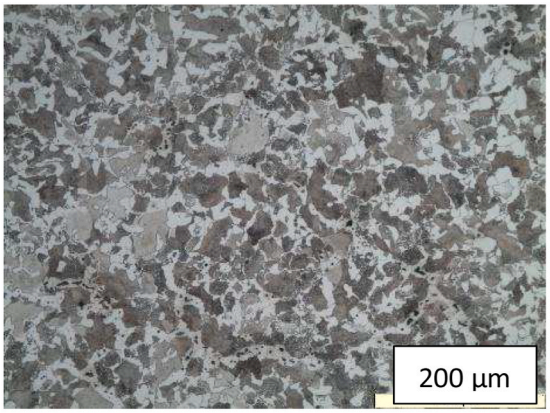
Sample 3 (D=13.3 mm; magnification 20x)	Sample 4 (D=13.3 mm; magnification 20x)

Fig. 11. Work material microstructure in the longitudinal and transversal sections.

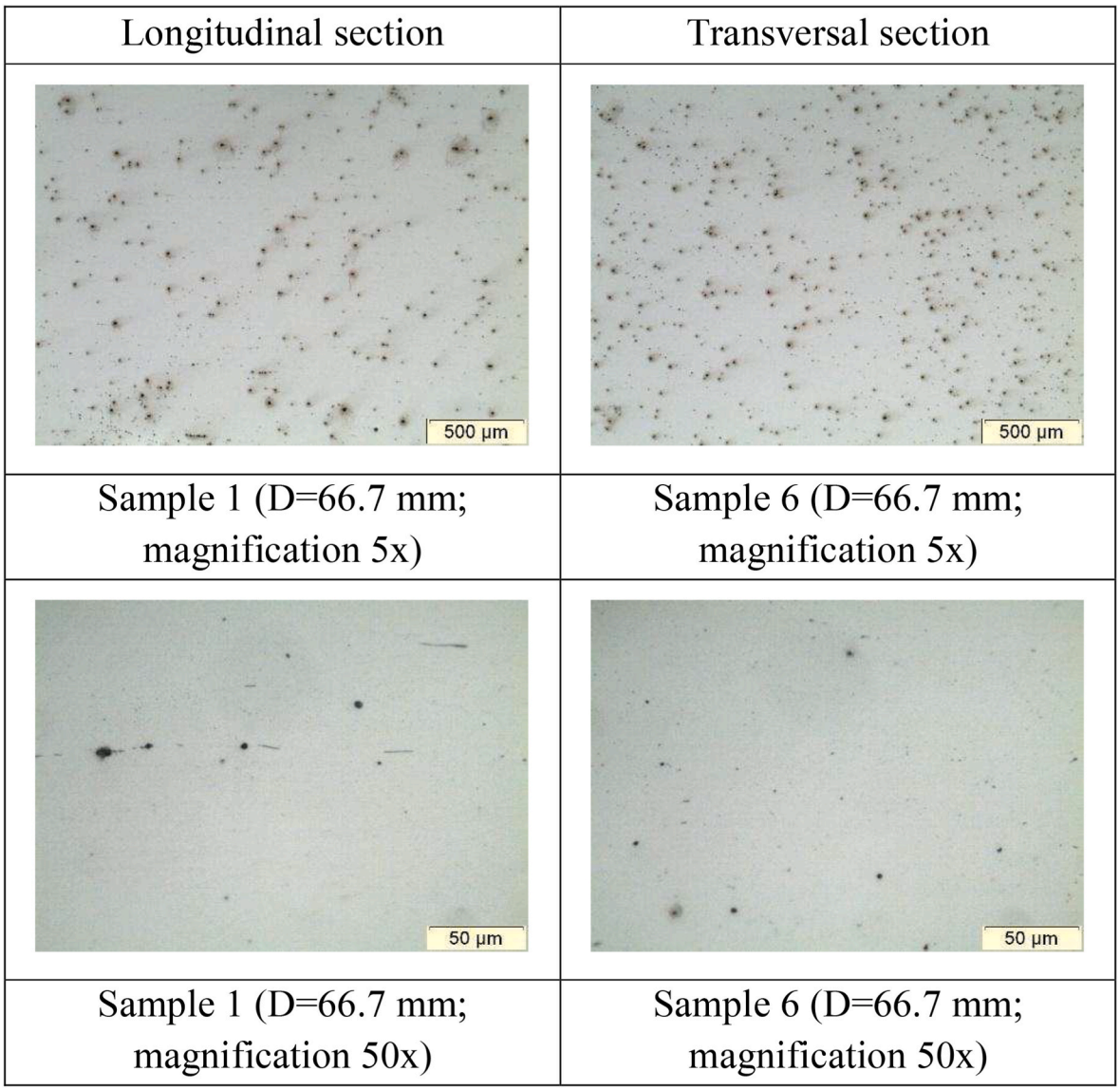

Fig. 12. Inclusions (black spot) observed in Sample 1 and Sample 6 at different magnifications.

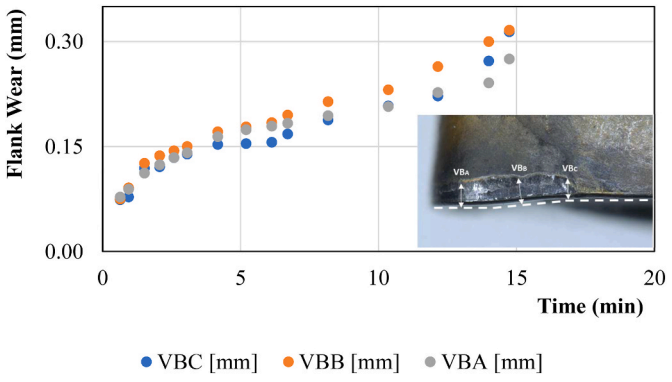

Fig. 13. Comparison among flank wear measured in three different zones of the flank surface ($v_c = 400\ m/min$, first repetition).

the flank wear values measured during the first repetition of the test performed with a cutting speed of 400 m/min. At the end of the test, the extension of the width of the flank wear land in the central zone (VB_B) is higher than the width of the flank wear land measured in the A (VB_A) and C (VB_C) zones.

Observing the tool wear evolution of the test performed with a cutting speed $v_c = 400$ m/min (Fig. 14), it is possible to state that initially the extension of the flank wear width is regular and equal in the three considered zones. In fact, up to 10.3 min (Fig. 14c) of cut the values of VB_A, VB_B, and VB_C are very close (see also graph of Fig. 13). Starting form 10.3 min, VB_B increases faster than VB_A and VB_C. After 14.7 min (Fig. 14d) of cut, that corresponds to the end of the tool-life of this test, the difference between VB_B, and VB_A and VB_C is evident. For all the tests, it was observed that VB_B is the wear parameter that firstly reaches the limit of 0.3 mm. For this reason, VB_B was selected as tool wear parameter for building the tool wear versus time diagrams. The dominant wear mechanism during the tests was abrasion, but in the final phase of the tests also adhesive wear occurred (as visible in Fig. 14d). In the accelerated wear zone, the cutting edge is widely rounded and the actual rake angles become negative, promoting built up edge phenomena.

Once the adhesion alters the geometrical features of the tools only at the end of the tool life, we consider this mechanism secondary as compared to abrasion. Fig. 15 shows the evolution of the wear on the tool rake face, for the first repetition of the test performed with a cutting speed $v_c = 400$ m/min. Similarly, wear development was observed on all the other tests, regardless the cutting speed.

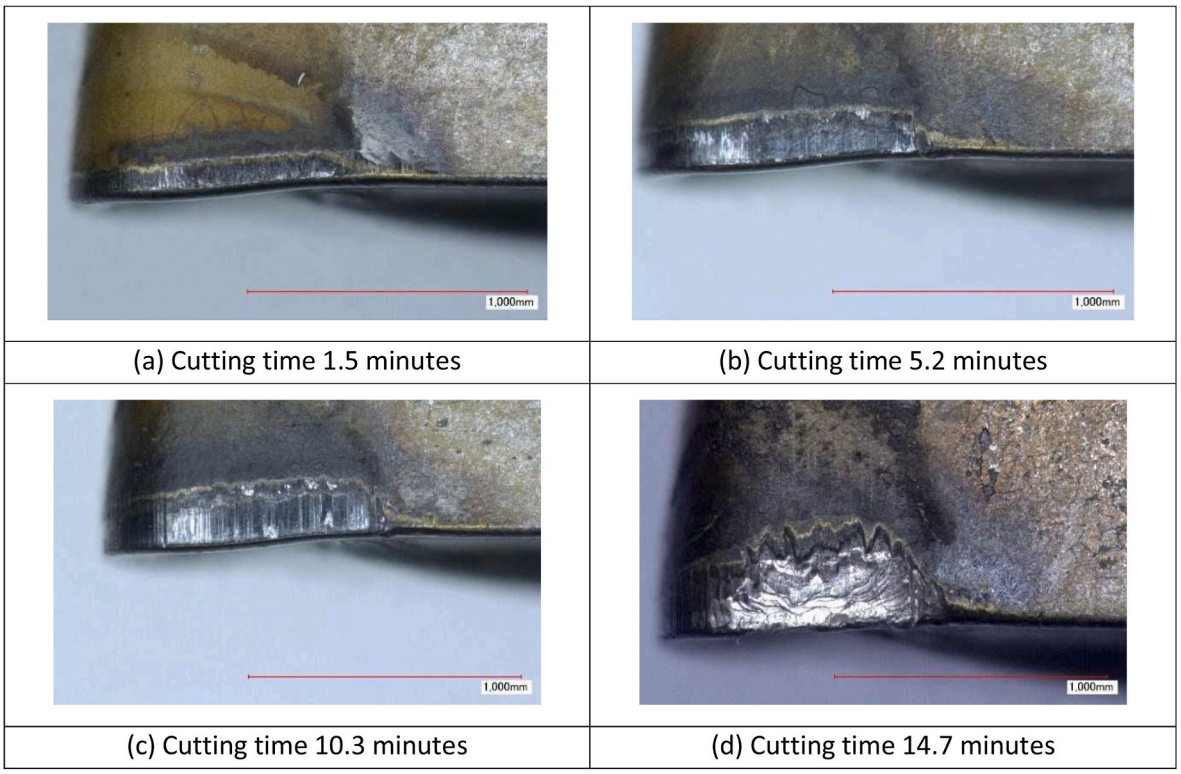

Fig. 14. Tool wear evolution ($v_c = 400\,m/min$, first repetition) (a) 1.5 min; (b) 5.2 min; (c) 10.3 min; (d) 14.7 min.

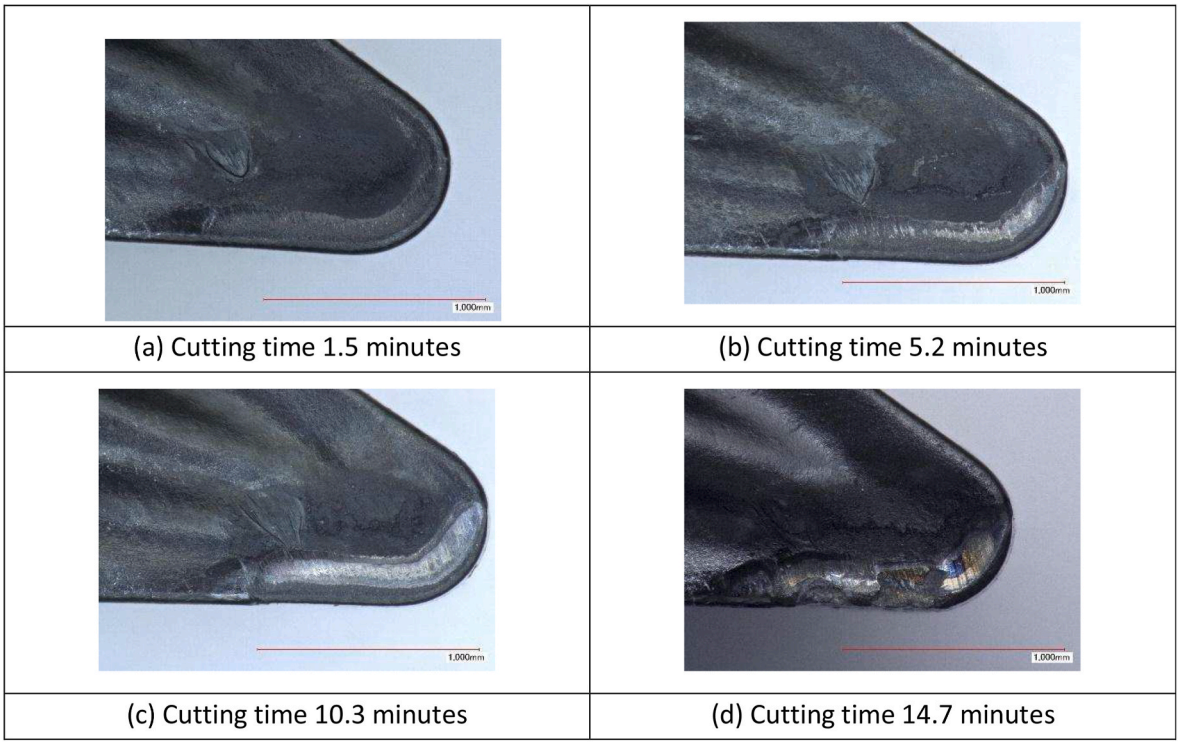

Fig. 15. Tool wear evolution on the tool rake face ($v_c = 400\,m/min$, first repetition) (a) 1.5 min; (b) 5.2 min; (c) 10.3 min; (d) 14.7 min.

4.2.2. Definition of the standard tool-wear curves

The collected tool wear data were used to define the coefficients of fitting curves representing the standard tool-wear curves. A polynomial function of the third order was used as a fitting model.

Fig. 16 shows three dataset (Exp1, Exp2, and Exp3) of the tool-life tests generated using a cutting speed $v_c = 400$ m/min, and the corresponding empirical model curve (red line in Fig. 16), the upper and lower bounds (dotted lines in Fig. 16). Upper and lower bounds were obtained respectively adding to and subtracting from the empirical model two times the deviation standard. The first repetition, performed

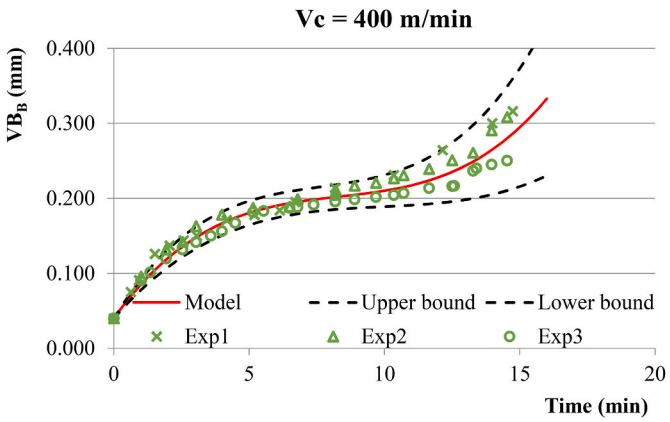

Fig. 16. Experimental tool wear data, fitting model, upper and lower bounds for test $v_c = 400\ m/min$.

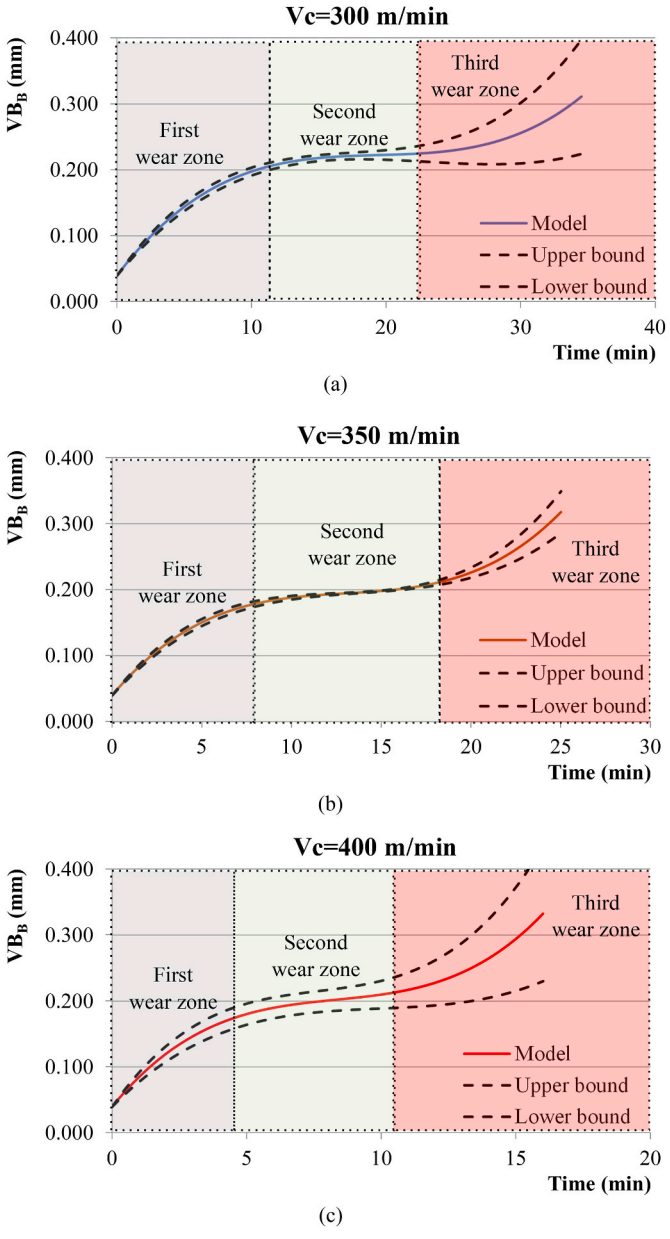

Fig. 17. Fitting model, upper and lower bounds for: a) $v_c = 300\ m/min$; b) $v_c = 350\ m/min$; c) $v_c = 400\ m/min$.

on lathe Sonim T9, does not significantly changes as compared to the others, performed on lathe OCN-PPL Olimpus. Analogue observations are valid for the tests performed with the cutting speed $v_c = 300$ m/min and $v_c = 350$ m/min. The features of the lathe did not influence the wear on the tool, the data can be statistically analysed regardless the machine as consequence.

Fig. 17 shows the fitting model curves, the upper and lower bounds of each tool-life test condition. All these curves showed the typical trend of wear curves as discussed in the introduction. The three wear zones are highlighted in the plots. As noticeable from these figures, all the plots do not start from the origin of the axis. This is due to the presence of a cutting edge radius equal to 0.04 mm on the unworn insert. The international standard ISO 3685 indicates to use the cutting edge as reference for the measurements of the width of flank land. Since the actual cutting edge is rounded, the nominal edge was used as reference, instead of the beginning of the flank surface. The usage of this reference increases the accuracy of the measurements: the position of the beginning of the flank is not constant because it shifts due to wear. On the other hand, the position of the nominal cutting-edge is constant during the machining, guaranteeing a reliable reference for the measurements of the width of the land. Considering a tool-life criterion limit of 0.3 mm, from the tool wear versus time graphs of Fig. 17, it is possible to estimate a useful tool-life equal to 33.8 min for the 300 m/min constant cutting speed tests, equal to 24.3 min for the 350 m/min constant cutting speed tests, and equal to 15.2 min for the 400 m/min constant cutting speed tests. As expected, as the cutting speed increases, the tool-life decreases. The constants of the Taylor's wear model are equal to C = 1085 and n = 0.362. They were computed by calculating the logarithm of cutting speed and tool life values. The data were interpolated with the best fitting linear relation ($r^2 = 0.98$), and constant n was calculated as the opposite of the inverse of the slope. Once n was known, it was used to compute a value of C for each of the three couples of cutting speed and tool life. Finally, an average value of C = 1085 was computed. Observing the trend of the upper and lower bounds, it is possible to deduce that the scattering of the experimental data is very low, independently to the cutting speed in the wear zones I and II. Differently, the wear zone III shows high data scattering and low repeatability for all the cutting speeds. This behaviour is expected since when the tool wear reaches the wear zone III, the degradation becomes unstable.

Equation from 2 to 4 report the expression of the empirical models representing the tool wear in function of the time for $v_c = 300$ m/min, $v_c = 350$ m/min, and $v_c = 400$ m/min, respectively.

Table 2
Cumulative tool wear tests data.

Test ID	Cutting speed (m/min)	*Interval time (min)*	Starting value of VB (mm)	Final value of VB (mm)	Estimated useful tool-life (min)
A	400	6min 15s	0.000	0.190	21.25
	300	10min 15s	0.190	0.220	
	350	End of tool-life	0.220	>0.300	
B	350	5min	0.000	0.150	19
	400	10min	0.150	0.250	
	300	End of tool-life	0.250	>0.300	
C	300	4min 15s	0.000	0.130	22.50
	350	8min 45s	0.130	0.195	
	400	End of tool-life	0.195	0.300	
D	400	4min 30s	0.000	0.175	31
	350	11min 30s	0.175	0.220	
	300	End of tool-life	0.220	>0.300	

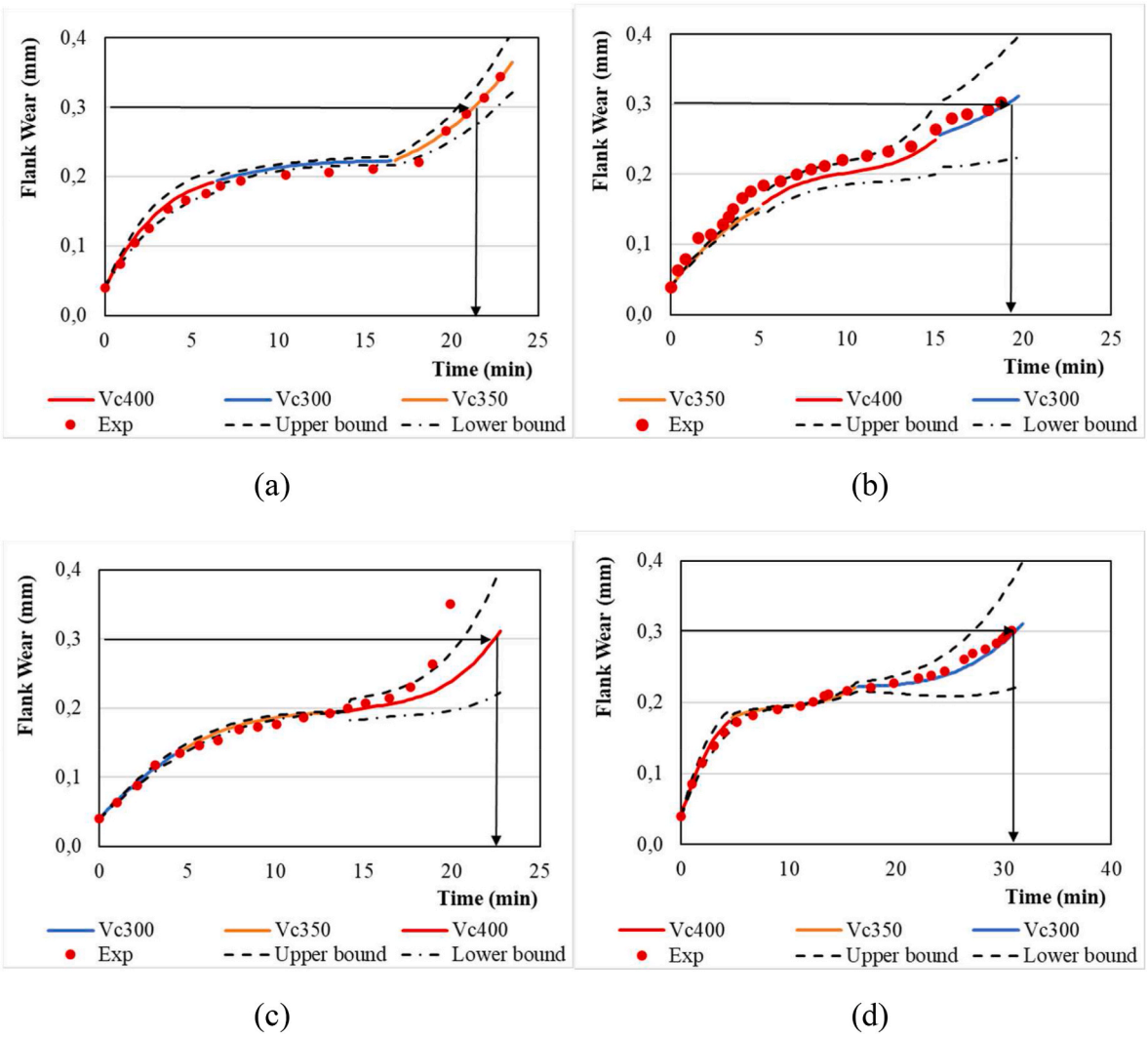

Fig. 18. Theoretical cumulative tool-wear curves and VCS experimental values; a) test A; b) test B; c) test C; d) test D.

$$VB_{B\_300} = 0,00002346 \bullet T^3 - 0,00136704 \bullet T^2 + 0,02710470 \bullet T + 0,04 \quad (2)$$

$$VB_{B\_350} = 0,00006076 \bullet T^3 - 0,00237304 \bullet T^2 + 0,03246927 \bullet T + 0,04 \quad (3)$$

$$VB_{B\_400} = 0,00022124 \bullet T^3 - 0,00553757 \bullet T^2 + 0,05025645 \bullet T + 0,04 \quad (4)$$

All the equations have the same constant term that corresponds to the cutting edge radius of the unworn insert.

4.2.3. Cumulative tool-wear curve building and estimation of the tool-life

Four VCS tool-life tests were designed varying the cutting speed during the same test, and the theoretical cumulative tool wear curves were built applying the procedure described in Section 2 to the tool wear curves reported in Section 4.3.2. In VCS tests, the depth of cut, feed, and metal cutting fluid were set as in the standard tool wear tests. Table 2 shows the sequences of cutting speed and the corresponding tool wear intervals. It reported also the theoretical useful tool-life of each cumulative tool wear sequence. Tool life was estimated using equations from 2 to 4 and by considering a tool-life criterion of 0.3 mm.

Fig. 18 shows a comparison between the predicted tool wear using the four empirical cumulative tool-wear equations designed as described in Table 2 and the measured tool wear achieved during VCS tests. The empirical curves are represented with coloured lines (blue for 300 m/min, orange for 350 m/min, red for 400 m/min), while the red dots visible in the graphs of Fig. 18 are the tool wear values measured during the experimental tests performed doing the sequences reported in Table 2. To consider the variability of the VB data, the upper and lower limit visible in Fig. 18 were added to the theoretical curves. They are represented by dotted lines (upper bound) and dash-dotted lines (lower bound). The validity of the cumulative procedure is ensured by the positioning of the red dots between the upper and lower limits of the analytical model, independently of the cutting speed sequence.

The agreement between the experimental results and the empirical curves is remarkable, confirming the validity of the proposed procedure. In particular, in the wear zones I and II there is a full matching between measured and predicted tool wear. A low discrepancy can be observed in the wear zone III, but as already discussed this behaviour is normal since in this zone the tool wear changes significantly, and the model is affected by high uncertainty (Fig. 18). The occurrence of adhesion wear in wear zone III increases the variability of the width of the flank land, since this phenomenon is less repeatable than abrasion wear.

4.3. Cutting force

The current section illustrates the resulted achieved in terms of forces and, in particular, how the force components depend on the wear.

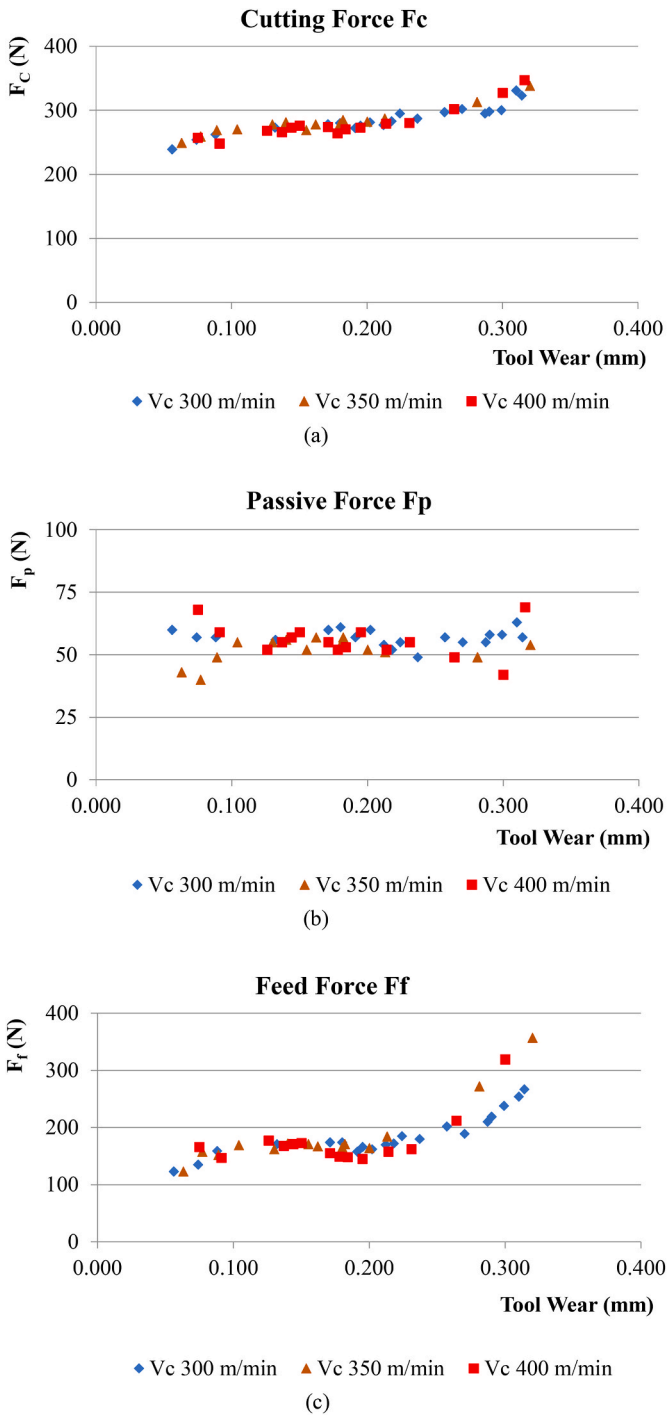

Fig. 19. Force versus tool-wear, (a) cutting force component; (b) passive force component; (c) feed force component.

Fig. 19 shows the cutting (Fig. 19 (a)), the passive (Fig. 19 (b)), the feed (Fig. 19 (c)) force components versus the width of the flank land, measured during the first repetitions of each CCS test. Analogue results were achieved during the second and third repetitions of the tests, but data can not be easily represented because the cutting force measurements were done in correspondence of different flank land width. The cutting force component trend is related to the wear zone: when the tool is new, the cutting force is slightly lower than in the steady state phase. Subsequently, during the wear zone II the cutting force is constant. As expected, when the tool wear reaches the wear zone III, the cutting force values increase due to the high deterioration of the cutting tool due to the abrasive and adhesive wear. The passive force components resulted less influenced by the tool wear, while feeding force has a trend comparable with the cutting speed. Furthermore, the increase of feeding force in wear zone III is higher than the increase of cutting force in the same instants.

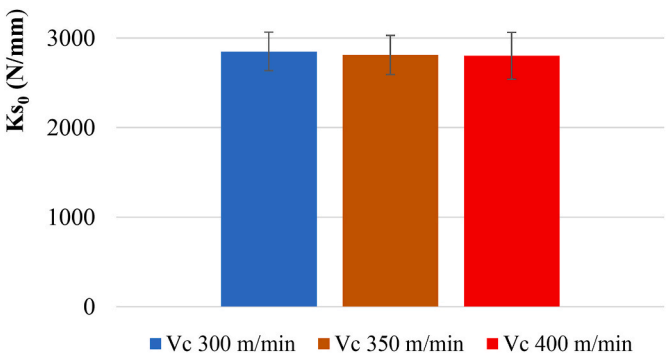

Fig. 20. Specific cutting pressure versus cutting speed.

As well known, the cutting force is mainly affected by depth of cut and feed. Cutting speed ranging in conventional parameter space has a minor impact on cutting force during machining of steels. The low difference between cutting speeds is determined by the process, which cannot be performed achieving successful results with lower or higher speeds. The weak relation between forces and cutting speed is confirmed by the experimental data. In fact, as shown in Fig. 19, measured cutting forces are independent of the cutting speed, for the same value of VB.

These results are confirmed by Fig. 20, which reports the specific cutting force as a function of the cutting speed. This parameter was calculated normalising the mean cutting force over the uncut chip cross section. From Fig. 20, it is possible to state that the cutting speed range considered in the experimental tests is characterised by similar values of the specific cutting force. The comparability between specific cutting forces ensures that built up edge (BUE) phenomena did not occur, also at the minimum cutting speed. In fact, the presence of built up edge determines an increasement of the actual cutting edge radius, with a consequent reduction of the cutting edge sharpness and an increasement of specific cutting force. These observations support the validity of the procedure to test cumulative tool wear by varying cutting speed and by combining the empirical curves of VB to predict the actual evolution of wear and the tool-life.

5. Conclusions

In this paper a research study to develop a robust procedure to predict the tool-life of a tool employed with different cutting speeds (i.e., under cumulative tool wear effect) was developed. The methodology can be applied to industrial context, where the employment of different cutting speeds during machining operations frequently occurs. The proposed procedure goes beyond the limits of the international standards and the methodologies found in literature [22–24], since the non-linear correlation between tool wear and cutting time is considered. Starting from tool wear curves obtained by standard tool-life tests at constant cutting speed, the empirical tool-life curve for a given machining cycle based on different cutting speed is built. This curve is then utilized to predict the tool-life under cumulative tool wear conditions.

To validate the proposed procedure, several machining cycles representing different cumulative tool wear conditions were designed and performed on AISI 1045. A proper characterization of the working material and the tools validated the results of the research, excluding that hardness and microstructure had influenced the outputs of this study. The repetitions of the tests and the statistically based approach allowed to highlight the effects of the variability of damage phenomena. For each

cycle the corresponding empirical tool wear curve was constructed. The comparison between experimental and predicted tool wear curves demonstrated the full validity of the proposed procedure.

CRediT authorship contribution statement

Andrea Abeni: Writing – original draft, Visualization, Methodology, Investigation, Formal analysis, Data curation, Conceptualization. **Aldo Attanasio:** Writing – original draft, Visualization, Project administration, Methodology, Investigation, Funding acquisition, Formal analysis, Data curation, Conceptualization. **José Outeiro:** Writing – review & editing, Supervision, Project administration, Methodology, Funding acquisition, Conceptualization. **Gerard Poulachon:** Writing – review & editing, Supervision, Project administration, Methodology, Funding acquisition, Conceptualization.

Declaration of competing interest

The authors declare that they have no known competing financial interests or personal relationships that could have appeared to influence the work reported in this paper.

Acknowledgments

The authors of this paper gratefully acknowledge Ascométal France Holding SAS for providing the material, the Eng. Alessandro Metelli, Eng. Marcon Bertrand for the support to the experimental activities. Financial support was provided by the international research program “Galileo” 2021 n°G21_152 /46487NM financed by Università Italo Francese/ Université Franco Italienne (UIF/UFI).

Data availability

Data will be made available on request.

References

[1] M. Schreiber, N. Weisbrod, A. Ziegenbein, J. Metternich, Tool management optimisation through traceability and tool wear prediction in the aviation industry, J. Inst. Eng. Prod. 17 (2) (2023) 185–195.
[2] A.R.F. Oliveira, L.R.R. Da Silva, V. Baldin, M.P.C. Fonseca, R.B. Silva, A. R. Machado, Effect of tool wear on the surface integrity of Inconel 718 in face milling with cemented carbide tools, Wear 476 (2021) 203752.
[3] N. Troß, J. Brimmers, T. Bergs, Tool wear in dry gear hobbing of 20MnCr5 case-hardening steel, 42CrMo4 tempered steel and EN-GJS-700-2 cast iron, Wear 476 (2021) 203737.
[4] ISO - ISO 3685, Tool-life testing with single-point turning tools (1993). https://www.iso.org/standard/9151.html.
[5] ISO - ISO 8688–1, Tool-life testing in milling — Part 1: face milling. https://www.iso.org/standard/16091.html, 1989.
[6] ISO - ISO 8688–2, Tool-life testing in milling — Part 2: end milling. https://www.iso.org/standard/16092.html, 1989.
[7] N. Uçak, K. Aslantas, A. Çiçek, Experimental evaluation of tool wear and surface roughness under different conditions in high-speed turning of Ti6Al4V alloy, Journal of Materials and Manufacturing 2 (1) (2023) 1–10.
[8] C. Cappellini, A. Abeni, Development and implementation of crater and flank tool wear model for hard turning simulations, Int. J. Adv. Des. Manuf. Technol. 120 (3) (2022) 2055–2073.
[9] A. Attanasio, E. Ceretti, J. Outeiro, G. Poulachon, Numerical simulation of tool wear in drilling Inconel 718 under flood and cryogenic cooling conditions, Wear 458 (2022) 203403.
[10] M. Marani, M. Zeinali, V. Songmene, C.K. Mechefske, Tool wear prediction in high-speed turning of a steel alloy using long short-term memory modelling, Measurement 177 (2021) 109329.
[11] S. Bombiński, J. Kossakowska, K. Jemielniak, Detection of accelerated tool wear in turning, Mech. Syst. Signal Process. 162 (2022) 108021.
[12] A. Abeni, C. Cappellini, A. Attanasio, Finite element simulation of tool wear in machining of nickel-chromium based superalloy, Proc. ESAFORM 4302 (2021).
[13] Z. Punta, T. Hrynievicz, Advanced model of the tool edge blunting under machining, Int. J. Adv. Manuf. Technol. 51 (2010) 35–43.
[14] J. Kundrák, Surface layer microhardness changes with high speed turning of hardened steels, Int. J. Adv. Manuf. Technol. 53 (2010) 105–112.
[15] A.J. Fernández-Abia, J. Barreiro, L.N. López de Lacalle, Effect of very high cutting speeds on shearing, cutting forces and roughness in dry turning of austenitic stainless steels, Int. J. Adv. Manuf. Technol. 57 (2011) 61–71.
[16] A. Attanasio, E. Ceretti, A. Fiorentino, C. Cappellini, C. Giardini, Investigation and FEM-based simulation of tool wear in turning operations with uncoated carbide tools, Wear 269 (2010) 344–350.
[17] P.C. Wanigarathne, A.D. Kardekar, O.W. Dillon, G. Poulachon, I.S. Jawahir, Progressive tool-wear in machining with coated grooved tools and its correlation with cutting temperature, Wear 259 (7–12) (2005) 1215–1224.
[18] M.A. Miner, Cumulative damage in fatigue, ASME J Appl Mech 67 (1945) A159–A164.
[19] Z. Palmai, Anwendung der Taylorschen Gleichung auf die Zerspanung mit wechselnd sich ändernden Schnittgeschwindigkeiten, Arch. für das Eisenhuttenwes. 49 (2) (1978) 89–93.
[20] Z. Pálmai, Cutting tool-life in machining at various speeds, Key Eng. Mater. 581 (2014) 38–43.
[21] Z. Pálmai, A model of non-linear cumulative damage to tools at changing cutting speeds, Int. J. Adv. Des. Manuf. Technol. 74 (2014) 973–982.
[22] K. Jemielniak, M. Szafarczyk, J. Zawistowski, Difficulties in tool-life predicting when turning with variable cutting parameters, CIRP Annals 34 (1) (1985) 113–116.
[23] N.P. Hung, C.H. Zhong, Cumulative tool wear in machining metal matrix composites Part I: modelling, J. Mater. Process. Technol. 58 (1) (1996) 109–113.
[24] D.K. Ojha, U.S. Dixit, An economic and reliable tool-life estimation procedure for turning, Int. J. Adv. Des. Manuf. Technol. 26 (7) (2005) 726–732.
[25] P. Albertelli, V. Mussi, M. Monno, Development of generalized tool-life model for constant and variable speed turning, Int. J. Adv. Des. Manuf. Technol. (2022) 1–17.